FACILE AND ONE-STEP SYNTHESIS OF ZIRCONIUM OXIDE NANOPARTICLES FOR REMOVAL OF PHOSPHATE AND LEAD(II) IONS

Lim Dillion (3S3), Bryan Lee Chong Han (3P1), Ho Shanley (3P1)

Group 1-23

Abstract

Water pollution, caused by toxic pollutants such as lead(II) and phosphate ions, results in a lack of safe drinking water. Zirconium oxide nanoparticles show great promise as an adsorbent in water purification. However, the conventional method of synthesizing zirconium oxide nanoparticles involves calcination. Although it is effective, it is extremely energy-intensive and economically unfriendly. In the present study, zirconium oxide was synthesized using a facile precipitation method using zirconium oxychloride, sodium hydroxide and banana peel extract. The zirconium oxide nanoparticles synthesized were evaluated in terms of their adsorption capabilities on lead(II) and phosphate ions and by varying the initial concentration and pH of phosphate and lead(II) ion solutions. Results showed that zirconium oxide nanoparticles synthesized using banana peels are spherical in shape and have a significantly lower diameter than that without banana peel extract. Zirconium oxide nanoparticles are also comparable to calcium oxide (lime) and commercial activated carbon in the removal of phosphate and lead(II) ions respectively, removing 99.7% of phosphate ions and 99.5% lead(II) ions. The simple, one-step proposed method of synthesizing zirconium oxide could potentially reduce cost of synthesis of zirconium oxide, rendering its use to purify water feasible.

1. Introduction

Due to agricultural pollution, natural solubilization of rocks and industrial wastewater discharge, the high phosphate concentration in natural water has been a big threat to the environmental system (Bai, Yuan, Ji, & Yan, 2018). Excess phosphate in water bodies could result in eutrophication which is harmful to aquatic life and deteriorates water quality, and even have a hazardous influence on humans. Phosphate often causes fatal cardiovascular calcification because it leads to the deposition of calcium phosphate crystals in various tissues (Razzaque, 2011).

Another pollutant commonly found in water is lead(II) ions which may cause many serious disorders like anemia, kidney diseases, nervous disorders and even deaths (Naseem, 2012). Infants and young children are especially sensitive to even low levels of lead, which may contribute to behavioural problems, learning deficits and lowered IQ (Wani, Ara, & Usmani, 2015).

Conventional phosphorus removal methods from wastewater include chemical precipitation, biological processes, reverse osmosis and sorption processes (Jiang & Wu, 2010). On the other hand, current treatment methods for removal of lead(II) ions from industrial wastewater include chemical precipitation, ion exchange, membrane separation, and adsorption (Dakhil, 2015). Among these techniques, adsorption is a promising method to treat wastewater containing both phosphate and lead(II) ions, due to its high efficiency, low cost and ease of carrying out (Keiteb, Saion, Zakaria, & Soltani, 2016). Although activated carbon is the most popular adsorbent used throughout the world for the removal of pollutants, its generation is difficult and is costly, which restricts its application in developing countries (Kyriakopoulos & Doulia, 2006).

Zirconium oxide has been increasingly researched upon in recent years, with applications including artificial jewellery, insulating materials, light shutters and stereo television glasses. According to Wang, Liu, Chen and Li (2012), zirconium oxide nanoparticles have high adsorption capacities for metal ions, even with extremely high concentrations of competing ions, hence being a promising adsorbent for industrial wastewater treatment. In addition, zirconium loaded materials such as zirconium loaded reduced graphene oxide (Luo et al., 2016) and zirconium loaded activated carbon (Wajima, 2016) have a relatively strong affinity for phosphate. As zirconium oxide is very resistant to acids, alkalis, oxidants, and reductants (Suzuki, Bomani, Matsunaga, & Yokoyama, 2000), it is a promising adsorbent for both phosphate and lead(II) ions.

Based on several studies (Keiteb et al., 2016; Salehpour & Ghanbary, 2016), the conventional way of synthesising zirconium oxide nanoparticles involves calcination, which is highly energy-intensive and hence limits its use as an adsorbent.

Hence, this study aims to investigate the synthesis of zirconium oxide nanoparticles using a facile, simple and one-step synthesis via precipitation and the use of plant extracts as capping agents, and to evaluate the effectiveness of the synthesized zirconium oxide nanoparticles in removing phosphate and lead(II) ions.

2. Objectives and hypotheses

The objectives of this study are to

- To synthesize zirconium oxide via a precipitation reaction where banana peel extracts will provide biomolecules to stabilize the zirconium oxide nanoparticles

- To investigate the effectiveness of the synthesized zirconium oxide nanoparticles in adsorbing phosphate and lead(II) ions as compared to lime (a conventional chemical used to remove phosphate) and commercial activated carbon (a common adsorbent used to remove lead(II) ions).
- To study the effect of pH and initial concentration of phosphate and lead(II) ions on the percentage removal of the pollutants.

Hypotheses:

- The synthesized zirconium oxide nanoparticles are comparable to that of lime and commercial activated carbon in removing phosphate and lead(II) ions respectively.
- pH and initial concentration will affect the percentage removal of phosphate and lead(II) ions by zirconium oxide.

3. Materials and Methods

3.1 Materials

Sodium hydroxide, sodium dihydrogen phosphate and lead(II) nitrate were procured from GCE Chemicals. Zirconium oxychloride and Folin-Ciocalteau agents were purchased from Sigma Aldrich. Banana peels were obtained from local fruit stalls.

3.2 Preparation of banana peel extract

Banana peels were washed with deionised water, dried and blended. Dried banana peel (30 g) was then boiled with 100 ml of water for 15 minutes. The mixture was then filtered and stored at 4°C before use.

3.3 Total polyphenol content of banana extracts

The total phenolic content of banana peel was determined using the Folin-Ciocalteau assay with gallic acid as the standard (Song et al., 2010). An aliquot (1 ml) of banana peel extract was added to a 25 ml volumetric flask containing 9 ml of deionised water. A reagent blank using deionised water was also prepared. One milliliter of the Folin-Ciocalteau’s phenolic reagent was added to the mixture and shaken. After 5 min, 10 ml of 7% (w/v) sodium carbonate solution was added to the mixture. The solution was diluted to 25 ml with deionised water and mixed. After incubation for 90 min at room temperature, the absorbance against the prepared reagent blank was determined at 750 nm with an UV-VIS Spectrophotometer (Shimadzu UV1800). Calibration curve was prepared using gallic acid of concentrations of 20, 40, 60, 80 and 100 mg/l. The total phenolic contents of the extracts were expressed as milligrams of gallic acid equivalents (GAE) per kg of peel (mg GAE/kg).

3.4 Synthesis of zirconium oxide nanoparticles

With stirring, banana peel extract (1 ml) was added to aqueous zirconium oxychloride (0.3M). The pH of the mixture was adjusted to 7.5 with 1M sodium hydroxide, followed by vigorous stirring for 16 hours. The precipitate formed was centrifuged and washed with deionised water until the electrical conductivity of the supernatant was less than $1mScm^{-2}$. The final product was dried at 60°C until constant mass and ground into fine powder using a mortar and pestle. The reaction which leads to the formation of zirconium oxide nanoparticles is proposed to be:

$$ZrOCl_2 + 2NaOH \rightarrow ZrO_2 + 2NaCl + H_2O$$

Polyphenols present in banana peel extract act as capping agents to stabilize the nanoparticles by preventing them from aggregating.

The zirconium oxide nanoparticles synthesized were characterised using Scanning Electron Microscopy (SEM), Energy Dispersive Spectroscopy (EDS) and X Ray Diffraction (XRD).

3.5 Adsorption studies

3.5.1 Effect of initial concentration

The adsorbate solutions were prepared by dissolving different amount of AR grade NaH_2PO_4-H_2O and $Pb(NO_3)_2$ in deionized water respectively to achieve solutions of concentration ranging from 50 mg/L to 250 mg/L of phosphate or lead(II) ion. Batch adsorption studies were carried out with beakers containing 20 ml of phosphate or lead(II) ion solution of different concentrations and 0.10 g of zirconium oxide. The mixtures were stirred for 24 hours, after which they were centrifuged and the supernatant analysed for residual phosphate and lead(II) ion using a colorimeter (HACH DR 890) and an Atomic Absorption Spectrophotometer (Shimadzu 6300) respectively. The set-ups also included a control without any zirconium oxide. Five replicates were conducted for each concentration.

The equilibrium concentration data were fitted into Langmuir and Freundlich isotherms (Appendix, Pg 13-15) to determine the adsorption mechanisms.

Adsorption of phosphate and lead(II) ion was evaluated in terms of adsorption capacity (Q) and removal efficiency (R). The adsorption capacity (Q) was calculated in mg/g according to the following formula:

$$Q = \frac{(C_i - C_f)V}{M}$$

C_i = initial concentration; C_f = final concentration
V = volume of solution; M = mass of ZrO_2

Removal efficiency (R) was calculated in % according to the following formula:

$$R = \frac{(C_i - C_f)}{C_i} x100\%$$

C_i = initial concentration; C_f = final concentration

3.5.2 Effect of pH

Effect of pH on phosphate and lead(II) ion uptake can throw light on the mechanism of how zirconium oxide adsorbs both ions. The initial concentration of the pollutant ion was fixed at 50 mg /l and the mass of zirconium oxide was fixed at 0.1 g while the pH was varied between 2 to 12 for phosphate and pH 2 to 6 for lead(II) ions using dilute hydrochloric acid or sodium hydroxide.

3.5.3 Comparing the performance of zirconium oxide with lime and commercial activated carbon

The effectiveness of zirconium oxide was compared with lime, a conventional coagulant used to remove phosphate and with commercial activated carbon, a conventional adsorbent used to remove lead(II) ions.

4. Result and Discussions

4.1 Characterisation of zirconium oxide nanoparticles

4.1.1 SEM images of zirconium oxide nanoparticles

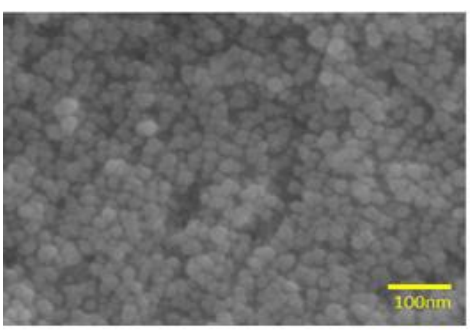

Figure 1: SEM image of zirconium oxide nanoparticles synthesized with banana peel extracts

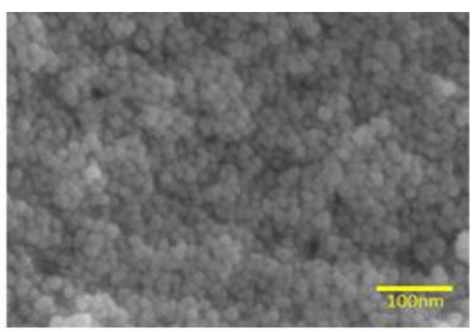

Figure 2: SEM image of zirconium oxide nanoparticles synthesized without banana peel extracts

Zirconium oxide nanoparticles synthesized were spherical in shape (figure 1). Using ImageJ, zirconium oxide nanoparticles synthesized without the banana peel extracts were determined to have an average size of 24.85 nm which is about twice as large as the ones synthesized with banana peel extract which have an average size of 12.18 nm (Figure 3). Total polyphenol test on banana peel extract shows that it contains 107 mg GAE/kg of peel which is comparable to most fruit peels such as blueberry and strawberry (Manach, Scalbert, Morand, Rémésy, & Jiménez, 2004). It was postulated that polyphenols present in the banana peel extract act as capping agents for the zirconium oxide nanoparticles (Figure 4), stabilizing them and preventing them from aggregating, hence resulting in particles with much smaller sizes

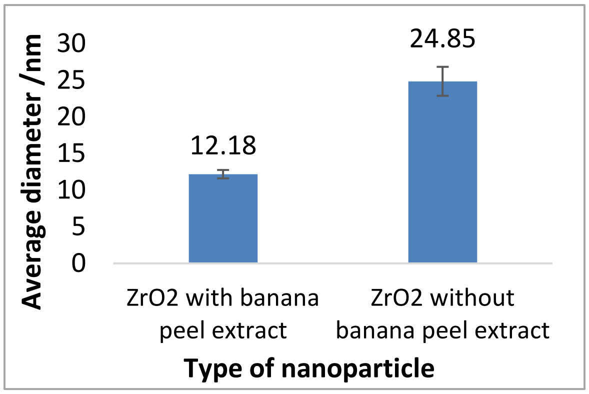

Figure 3: Diameter of zirconium oxide nanoparticles with and without banana peel extract

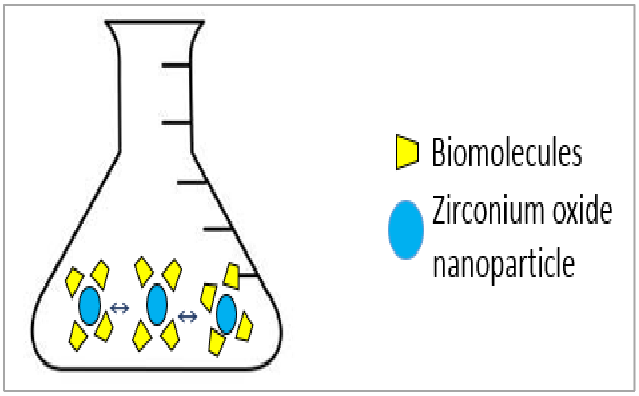

Figure 4: Polyphenols in plant extracts acting as capping and stabilizing agents for zirconium oxide nanoparticles

4.1.2 Energy-dispersive spectroscopy (EDS)

The presence of zirconium and oxygen confirms the identity of zirconium oxide. Carbon present is due to the polyphenols from the banana peel extract.

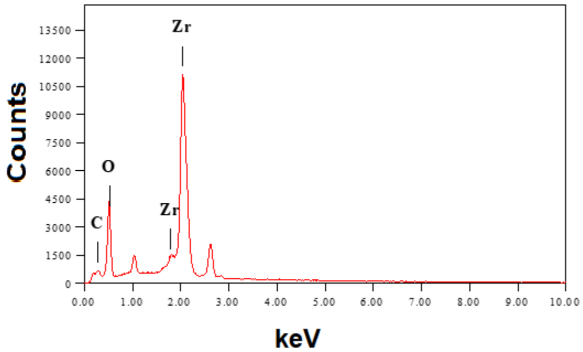

Figure 5: EDS of zirconium oxide nanoparticles synthesized

4.1.3 X-Ray Diffraction

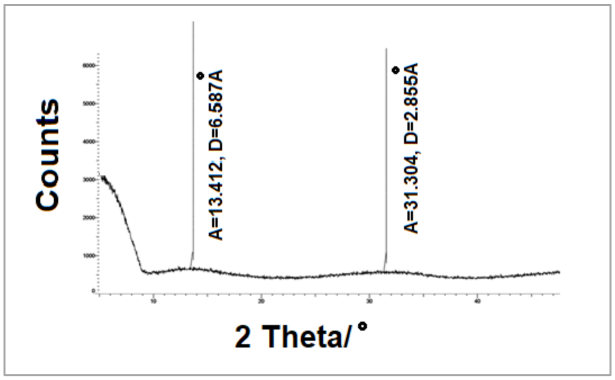

Figure 6: XRD pattern of zirconium oxide nanoparticles synthesized

The 2-theta peak at 31.3° (Figure 6) is characteristic of zirconium oxide. The XRD pattern of zirconium oxide synthesized is similar to those reported in literature (Keiteb, Saion, Zakaria, & Soltani, 2016). The broad peak indicates that the zirconium oxide is non-crystalline and amorphous.

4.2 Batch Adsorption studies

4.2.1 Comparison of adsorption of phosphate using ZrO_2 nanoparticles and CaO

Zirconium oxide is effective in adsorbing phosphate, removing more than 99% of phosphate (Figure 7). There is no significant difference in the percentage removal by zirconium oxide and lime as the p-value of Mann-Whitney test is 0.203 (>0.05). As illustrated by Figure 8, phosphate ions are being adsorbed via ion exchange with the surface hydroxyl groups present in zirconium oxide nanoparticles (Luo et al., 2016). On the hand, lime (CaO) removes phosphate via precipitation, as illustrated by the following equation:

$$10\ Ca^{2+}\ (aq) + 6\ PO_4^{3-}\ (aq) + 2OH^-\ (aq) \rightarrow Ca_{10}(PO_4)_6(OH)_2\ (s)$$

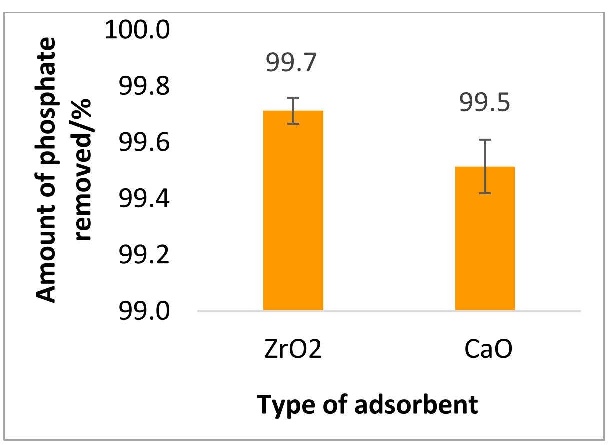

Figure 7: Adsorption of phosphate by zirconium oxide as compared to lime

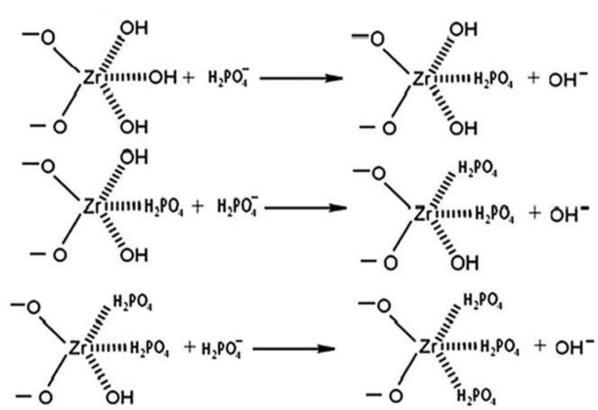

Figure 8: Adsorption of phosphate by zirconium oxide via ion exchange

4.2.2 Comparison of adsorption of Pb^{2+} using ZrO_2 nanoparticles and activated carbon

Zirconium oxide nanoparticles synthesized using banana peel extract removes close to 100% of lead(II) ions. There is no significant difference in the percentage removal of lead(II) ions by zirconium oxide and commercial activated carbon (p-value of Mann-Whitney test = 0.209 > 0.05)

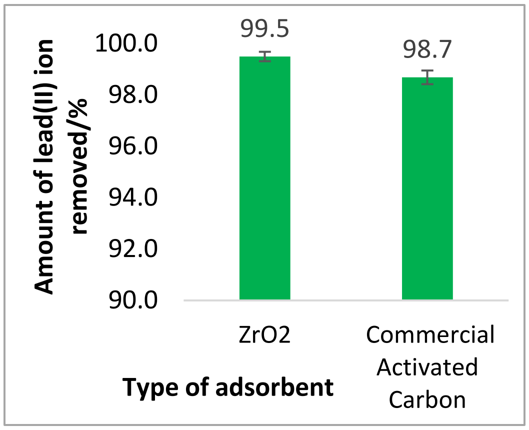

Figure 9: Adsorption of lead(II) ions by zirconium oxide as compared to commercial activated carbon

The high percentage of adsorption of lead(II) ions by zirconium oxide nanoparticles can be attributed to the ability of the hydroxyl groups present in zirconium oxide which could form dative bonds with the lead(II) ions (Yung et al., 2017), hence removing them from solution.

Activated carbon contains functional groups such as hydroxyl, phenol, ether and lactone groups which render it effective in binding to metal ions via dative bonds (Chen & Shunnian, 2004).

4.3 Effect of pH on adsorption by ZrO_2 nanoparticles

4.3.1 Phosphate adsorption

The phosphate adsorption on ZrO_2 nanoparticles was evidently dependent on the pH (Figure 10). At low pH, the percentage of adsorption increased from pH 2 to pH 6, with the optimum pH being 6. As pH increases beyond 6, percentage adsorption drops. A low pH in the acidic region causes the adsorption capability to decrease because of electrostatic repulsion between the negatively-charged hydroxyl group and phosphate groups (Rodrigues et al., 2011).

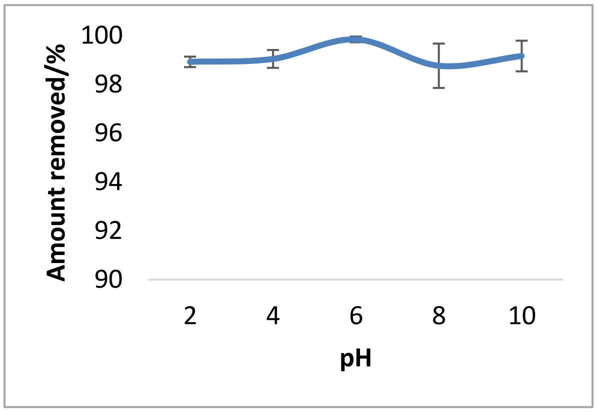

Figure 10: Effect of pH on adsorption of phosphate ions

However, at pH around 6, the predominant chemical species is $H_2PO_4^-$ (Figure 11) which has the same charge as hydroxyl groups, hence they are able to replace the hydroxyl groups favourably via ion exchange (Figure 11). This explains why the optimum pH for adsorption of phosphate is pH 6.

$$PO_4^{-3} + H_2O \rightleftharpoons HPO_4^{2-} + OH^-, \quad pK = 1.68$$
$$HPO_4^{-2} + H_2O \rightleftharpoons H_2PO_4^- + OH^-, \quad pK = 6.79$$
$$H_2PO_4^- + H_2O \rightleftharpoons H_3PO_4, \quad pK = 11.67$$

Figure 11: Predominant chemical species at different pK values

4.3.2 Lead(II) ions

The effect of pH on lead(II) ion adsorption by ZrO_2 nanoparticles was demonstrated in Figure 12. Under the acidic pH conditions, the adsorption performance increased significantly from pH 2 to pH 6. To avoid the spontaneous precipitation of lead(II) hydroxide, pH beyond 6 was not tested. Evidently, the removal of lead(II) ions was severely confined at a low pH, which was caused by the protonation of the ZrO_2 nanoparticles, causing H^+ and Pb^{2+} ions to compete for adsorption sites, decreasing its adsorption capability (Su *et al.*, 2013). The optimal pH for adsorption is determined to be between pH 5 to 6.

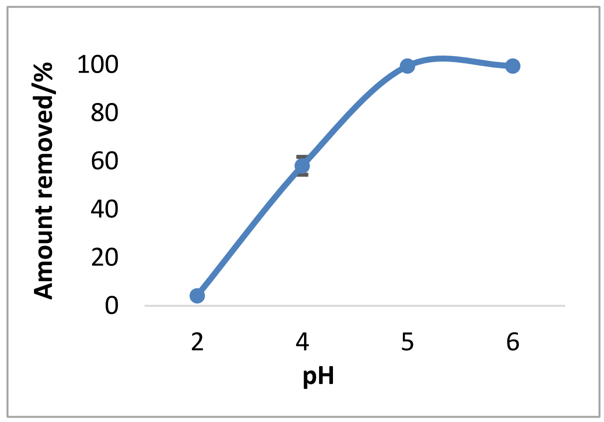

Figure 12: Effect of pH on adsorption of lead(II) ions

4.4 Isotherm Studies

The equilibrium concentration data of both phosphate and lead(II) ions fit Langmuir isotherms (Appendix, Pg 13-15), suggesting that the adsorption is monolayer on a homogeneous surface. Maximum adsorption capacities on phosphate and lead(II) ions were derived and compared with other adsorbents (Table 1 and 2). The maximum adsorption capacity (Q_{max}) of zirconium oxide on phosphate is higher than that on lead(II) ions. Compared to zirconium oxide without plant extracts and several other adsorbents reported in literature, the Q_{max} of zirconium oxide synthesized using banana peel extracts on both pollutants are higher, suggesting that it is an adsorbent with great potential to be used in water treatment.

Table 1 : Comparison of Maximum adsorption capacity of different adsorbents on phosphate

Adsorbent	Maximum adsorption capacity (mg/g)	Reference
Zirconium oxide with plant extract	106	This study
Iron hydroxide-Eggshell waste	14	Rodrigues *et al.*, 2014
Niobium oxide	13	
Red Mud Fe-Mn Binary oxide	1 23	
Zirconium oxide without plant extract	30	

Table 2 : Comparison of Maximum adsorption capacity of different adsorbents on lead(II) ions

Adsorbents	Maximum adsorption capacity (mg/g)	Reference
Zirconium oxide with plant extract	31.8	This study
Groundnut husk modified with guar gum	9.76	Ogunlalu *et al.*, 2017
Activated Carbon	26.6	
Pinewood Biochar	3.00	
Zirconium oxide without plant extract	25.0	Rahman et al., 2015

5. Conclusion and Future work

Zirconium oxide nanoparticles have been successfully synthesized using banana peel extracts via a simple and one-step precipitation reaction. Compared to zirconium oxide nanoparticles synthesized without banana peel extract, the ones synthesized using banana peel extracts are smaller in size. The zirconium oxide nanoparticles synthesized using banana peel extract are also comparable to conventional adsorbents, lime and activated carbon, in adsorbing phosphate and lead(II) ions respectively. Adsorption of phosphate and lead(II) ions by zirconium oxide is strongly dependent on pH. The optimum pH for adsorption of both phosphate and lead(II) ions is 6. The equilibrium experimental data is a good fit for Langmuir isotherm, suggesting that the adsorption of both phosphate and lead(II) ions by zirconium oxide is monolayer. The maximum adsorption capacity of zirconium oxide for phosphate and lead(II) ions was determined to be 106 mg g^{-1} and 32 mg g^{-1} respectively. The simple, one-step method of synthesizing zirconium oxide nanoparticles proposed in this study is a promising and more eco-friendly alternative to current method of synthesizing zirconium oxide nanoparticles, rendering the use of zirconium oxide in water filters more cost effective and feasible.

6. Future Work

Possible extensions to this study include investigating the kinetics of adsorption of phosphate and lead(II) ions by zirconium oxide. In real life, wastewater contains multiple anions and hence it would be relevant to study whether the presence of other anions would affect the adsorption of phosphate by zirconium oxide. Finally, for practical usage, zirconium oxide nanoparticles can be embedded into calcium alginate beads for easier retrieval and the possibility of reusability.

References

Bai, L., Yuan, L., Ji, Y. , & Yan, H (2018). Effective Removal of Phosphate from Aqueous by Graphene Oxide Decorated with αα-Fe_2O_3 αα-Fe_2O_3: Kinetic, Isotherm, Thermodynamic and Mechanism Study. *Arab J Sci Eng*, *43*(7), 3611-3620. Doi: https://doi.org/10.1007/s13369-018-3124-3.

Chen, J.P., & Shunnian. (2004). Acid/Base-Treated Activated Carbons: Characterization of Functional Groups and Metal Adsorptive Properties. *Langmuir*, *20*(6), 2233-2242.

Dakhil, I.B (2005). Adsorption of lead from industrial effluents using rice husk. *International Journal of Engineering and Management Research*, *5*(1), 109-116.

Jiang, J.Q., & Wu, L. (2010), Preliminary study of calcium silicate hydrate (tobermorite) as crystal material to recovery phosphate from wastewater. *Desalination and Water Treatment*, *23*(1-3), 49–54.

Keiteb, S., Saion, E., Zakaria, A. & Soltani, N. (2016). Structural and Optical Properties of Zirconia Nanoparticles by Thermal Treatment Synthesis. *Journal of Nanomaterials*, 2016, *1*, 1-6.

Kyriakopoulos, G., & Doulia, D. (2006). Adsorption of pesticides on carbonaceous and polymeric materials from aqueous solutions: A review. *Separation and Purification Reviews*, *35*, 97-191; 191.

Luo, X., Wang, X., Bao, S., Liu, X., Zhang, W. & Fang, T. (2016). Adsorption of phosphate in water using one-step synthesized zirconium-loaded reduced graphene oxide. *Scientific Reports*, *6*, 39108.

Manach, C., Scalbert, A., Morand, C., Rémésy, C. & Jiménez, L. (2004). Polyphenols: food sources and bioavailability. *American Journal of Clinical Nutrition*, *79*, 727– 747

Naseem Z., (2012). Lead Removal from Water by Low Cost Adsorbents: A Review. Pak. *J. Anal. Environ. Chem*., *13*, 1-8.

Ogunlala, O.U., Aderibigbe, A.D., Oluwasina, O.O., & Amoo, I.A. (2017). Adsorption studies of Pb^{2+} from aqueous solutions using unmodified and citric acid – modified Plantain (*Musa paradisiaca*) Peels. *IOSR Journal of Applied Chemistry*, *10*(2), 30-39.

Rahman, S., & Sathasivam, K.V. (2015). Heavy Metal Adsorption onto *Kappaphycus* Sp. From Aqueous Solutions: The Use of Error Functions for Validation of Isotherm and Kinetic models. *BioMed Research International*, *2015*, 126298, 1-13.

Razzaque, M. S. (2011). Phosphate toxicity: New insights into an old problem. *Medical Science*, *120*(3), 91-97.

Rodrigues, L.A., Maschio, L.J., Coppio, L.S.C, Thim, G.P., & Silva, M.L.C.P (2011). Adsorption of phosphate from aqueous solution by hydrous zirconium oxide. *Environmental Technology*, *33*(12), 1345-1351.

Salehpour, M., & Ghanbary, F. (2016). Synthesis of cellulose/zirconium oxide nanocomposite and the study of its activity in the removal of pollutants. *IIOABJ*, *7*(5), 401-408.

Song, F-L., Gan, R-Y., Zhang, Y., Xiao, Q., Kuang, L., & Li, H-B. (2010). Total Phenolic Contents and Antioxidant Capacities of Selected Chinese Medicinal Plants. *Int. J. Mol. Sci.*, *11*, 2362-2372. Doi:10.3390/ijms11062362

Su, Y., Cui, H., Li, Q., Gao, S., & Shang, J.K. (2011). Strong adsorption of phosphate by amorphous zirconium oxide nanoparticles. *Water Research*, *4*(7), 5018-5026.

Suzuki, T.M., Bomani, J.O., Matsunaga, H & Yokoyama, T. (2000). Preparation of porous resin loaded with crystalline hydrous zirconium oxide and its application to the removal of arsenic. *React. Funct. Polym*, *43*, 165-172.

Wang, C., Liu, X., Chen, J. P., & Li, K. (2012). Superior removal of arsenic from water with zirconium metal-organic framework UiO-66. *Scientific Reports*, *5*, 16613, 1-10.

Wajima, T. (2016). Phosphate Adsorption on Zirconium-Loaded Activated Carbon, and its Application for Phosphate Recovery from Deep Seawater. *International Journal of Chemical Engineering and Applications*, *7*, 6.

Wani, A., L., Ara, A., & Usmani, J. A. (2015). Lead toxicity: A review. *Interdisciplinary Toxicology*, *8*(2), 55-64.

Yung, A., Lim, S.F., Chua, D., Sanaullah., D., Baini, R., & Abdullah, M.O. (2017). Adsorption equilibrium for heavy metal divalent ions (Cu^{2+}, Zn^{2+}, and Cd^{2+}) into zirconium-based ferromagnetic sorbent. *Advances in Materials Science and Engineering*, *2017*, 1210673. Retrieved from https://doi.org/10.1155/2017/1210673

Appendix - Equilibrium adsorption isotherm studies on ZrO_2 nanoparticles

Adsorption of phosphate

The equilibrium concentration data was fitted into the Langmuir and Freundlich linearized isotherm models as given in Equation 1 and Equation 2, respectively:

$$\frac{C_e}{q_e} = \frac{1}{bq_m} + \frac{C_e}{q_m} \qquad \textbf{(1)}$$

$$\log(qe) = \log(K_F) + \frac{1}{n}\log(C_e) \qquad \textbf{(2)}$$

Where C_e refers to the equilibrium concentration of the pollutant (mg/L), q_e is the adsorption capacity (mg/g), Q_m is the maximum adsorption capacity (mg/g), b is the Langmuir constant, indicating the sorption intensity. K_F is a constant related to sorption capacity and n corresponds to sorption intensity.

The Langmuir model assumes that adsorbed material (such as lead(II) ions) is adsorbed over a homogenous adsorbent surface at a constant temperature. The Freundlich model, however, assumes that adsorption occurs over a heterogenous surface. If the equilibrium concentration data fits the Langmuir isotherm model, adsorption can be inferred to be monolayer. Important information such as the maximum adsorption capacity can be derived from the inverse of the gradient of the Langmuir linear equation. In contrast, if the equilibrium concentration data fits the Freundlich isotherm, adsorption can be inferred to occur on a heterogenous surface and adsorption is multilayer.

Figure 13 shows the linearized Langmuir plot, where its gradient was used to calculate the maximum adsorption capacity (Q_{max}), which are tabulated in Table 3. Figure 14 shows the linearized Freundlich plot. The correlation coefficients (R^2) indicate that the Langmuir model fits the adsorption data better. Maximum adsorption capacity on phosphate was determined to be 106 mg g^{-1}.

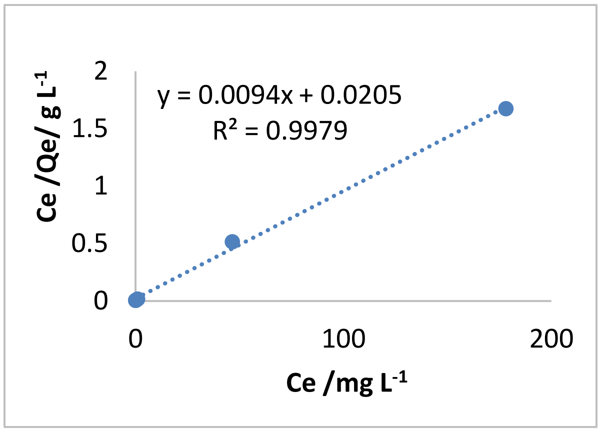

Figure 13: Langmuir isotherm for phosphate

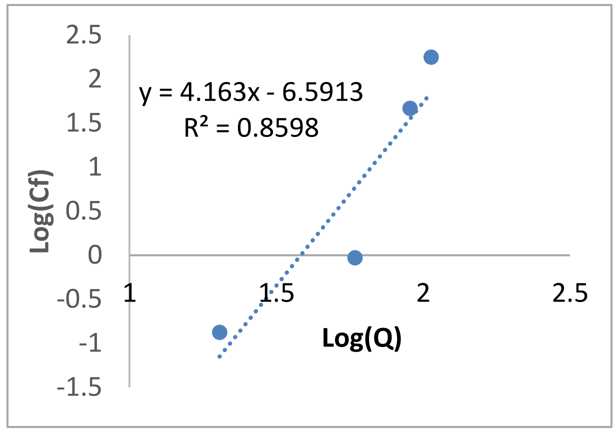

Figure 14: Freundlich isotherm for phosphate ions

Table 3: The isotherm parameters for the adsorption of phosphate ions by ZrO_2 nanoparticles

Pollutant	**Langmuir**			**Freundlich**
	Q_m (mg g^{-1})	**b (L mg^{-1})**	**R^2**	**R^2**
PO_4^{3-} ions	106	0.46	0.9979	0.8598

Adsorption of lead(II) ions

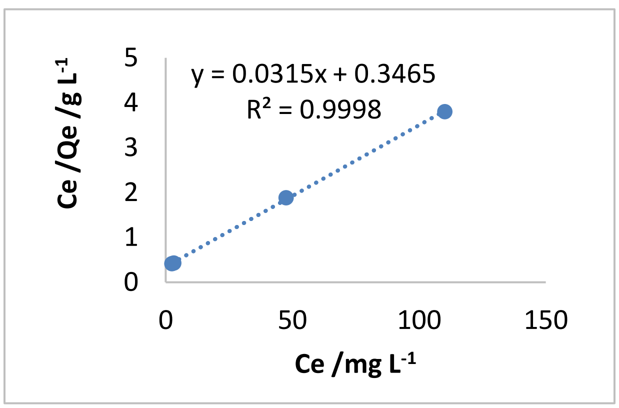

Figure 15: Langmuir isotherm for lead(II) ions

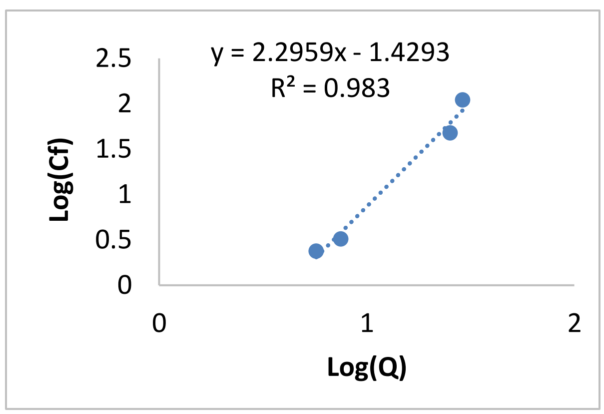

Figure 16: Freundlich isotherm for lead(II) ions

Figure 15 shows the linearized Langmuir plot, where its gradient was used to calculate the Qm (maximum adsorption capacity), which are tabulated in Table 4. Figure 16 shows the linearized Freundlich plot. The correlation coefficients (R^2) indicate that the Langmuir model again fits the adsorption data better. Maximum adsorption capacity on lead(II) ions was determined to be

31.8 mg g^{-1}.

Table 4: Isotherm parameters for the adsorption of Pb^{2+} ions by ZrO_2 nanoparticles

Pollutant	**Langmuir**			**Freundlich**
	Q_e (mg g^{-1})	**b (L mg^{-1})**	**R^2**	**R^2**
Lead(II) ions	31.8	0.08	0.9998	0.983